Accurate Analytical Delay Models for VLSI Interconnects *

Andrew B. Kahng and Sudhakar Muddu

UCLA Computer Science Department, Los Angeles, CA 90024-1596 USA
abk@cs.ucla.edu, sudhakar@cs.ucla.edu

Abstract

Elmore delay has been widely used to estimate the interconnect delays in the performance-driven synthesis and layout of VLSI routing topologies. For typical *RLC* interconnections, Elmore delay can deviate significantly (by up to 33% or more) from SPICE-computed delay, since it is independent of inductance. We develop an analytical delay model to incorporate inductance effects into the delay estimate. Our method achieves delay estimates that are within 10% of SPICE-computed delay across a wide range of interconnect parameter values. We also give two example applications of our new analyses: (i) a condition under which interconnect delays can be minimized by introducing controlled ringing, and (ii) an extension of the New Delay model for estimation of delay in interconnect trees.

1 Overview

Accurate calculation of propagation delay in VLSI interconnects is critical to the design of high speed systems. With the evolution of VLSI technology, transmission line effects now play an important role in determining interconnect delays and system performance. Various techniques have been proposed for the simulation of interconnects. These techniques are based on either *simulation techniques* or (closed-form) *analytical formulas*. Direct simulation tools such as SPICE give the most accurate insight into arbitrary interconnect structures, but are computationally expensive. Transient simulation of lossy interconnects based on convolution techniques is presented in [RP91, LK92]. Faster techniques based on moment computations are proposed in [RGP91, RBR92, SK93].

The above methods, being simulation-based, are all computationally too expensive to be

*This work was supported by NSF Young Investigator Award MIP-9257982.

used in the performance-driven synthesis and layout of interconnection topologies. Thus, Elmore delay [Elm48], which represents the first moment of the transfer function, is the most widely used delay model in the performance-driven routing of clock distribution and Steiner global routing topologies. The problem with the Elmore delay model is that it cannot accurately estimate the delay for RLC interconnect lines. A typical comparison of RC and RLC line response is shown in Figure 1. The 90% threshold delay for the RLC line is 288 ps, and for the RC line the delay is 358 ps. However, Elmore delay, which does not depend on line inductance, will yield the same delay estimate of 358 ps for both the RC and the RLC cases; we see that Elmore delay overestimates the delay time. More generally, we can observe that the Elmore delay formula gives good estimates if the interconnect lines are RC or overdamped, but gives overestimates for RLC lines or underdamped interconnects. This inaccuracy can be a serious impediment to current performance-driven routing methods which try to determine optimal interconnect segment lengths and widths (as well as driver sizes) based on Elmore delay. Clearly, the solutions obtained using Elmore delay estimates can be sub-optimal.

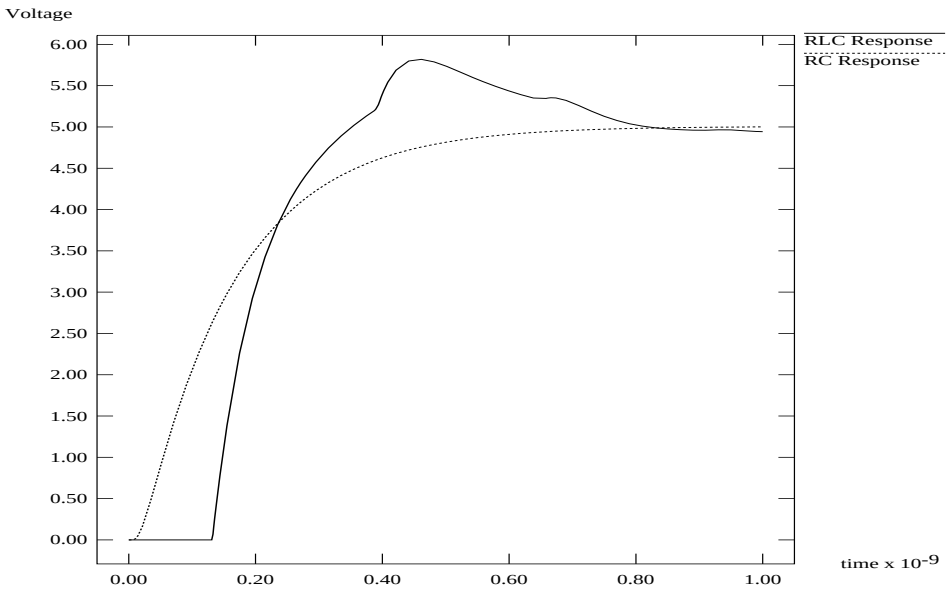

Figure 1: The difference between RC and RLC line delays. The interconnect line parameters are: $R = 0.075\ \Omega/\mu m$, $L = 0.123\ pH/\mu m$, $C = 8.8\ fF/\mu m$, and the length of the line is 400 μm. The driver resistance is 10.0 Ω and load capacitance is 2.0 pF.

The main contribution of this paper is a new and accurate *analytical* delay estimate for distributed RLC interconnects. Our formula stems from a two-pole analysis, and unlike previous

analytical delay formulas (i.e., Elmore delay) considers the effect of inductance in its delay estimate. The main distinction between our work and existing works lies in the dichotomy between simulation-based and analytic delay estimates. We also note that even though reduced-order moment-based approaches can potentially be used to compute the response within existing simulation tools (cf. works such as [RBR92, LK92]), none of these approaches has given any analytical delay estimation model, which is the key requirement in performance-driven routing and layout synthesis.

To experimentally validate our analysis and delay formula, we model VLSI interconnect lines having various combinations of source and load parameters, and obtain delay estimates by using SPICE, a two-pole simulator [Hor84, ZSTGC94], Elmore delay and the proposed analytical delay model. *The first two delay estimates are extracted from a computed response; the latter two are analytical (closed-form) expressions.* Over our range of test cases, Elmore delay estimates can be as much as 50% away from the SPICE-computed delays and do not have monotonic fidelity, i.e., the Elmore delay estimate can be either greater or less than than SPICE-computed delay. In contrast, the analytical delay model estimates are within 10% of SPICE delays, and always provide an upper bound on the actual (SPICE-computed) delay.

The rest of this paper is as follows. In Section 2 we review previous single-pole delay estimates for distributed RLC lines and Section 3 presents the analytical delay model for the distributed RLC line. Finally, Section 4 describes two sample applications of the analytical delay model, i.e., (i) we extend the model to obtain a delay estimate for general interconnection trees, and (ii) we obtain an explicit condition on the coefficients of the transfer function such that delay is minimized with controlled ringing (overshoot).

2 Previous Analytic Delay Models

The transfer function of an RLC interconnect line with source and load impedance (Figure 2) can be obtained using the ABCD parameters [Dwo79]

$$H(s) = \frac{V_2(s)}{V_0(s)} = \frac{1}{\left[\cosh(\theta h) + \frac{Z_S}{Z_0}\sinh(\theta h)\right] + \frac{1}{Z_T}\left[Z_0 \sinh(\theta h) + Z_S \cosh(\theta h)\right]} \qquad (1)$$

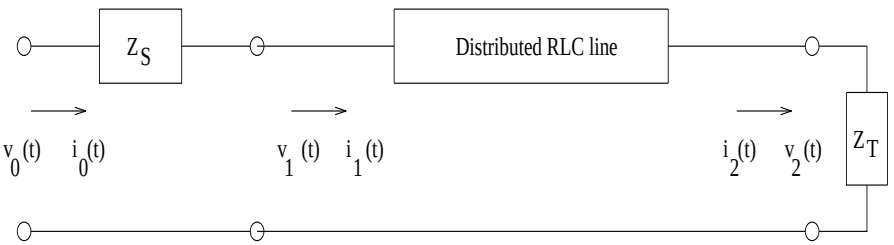

Figure 2: 2-port model of a distributed RLC line with source impedance Z_S and load impedance Z_T.

where propagation constant $\theta = \sqrt{(r+sl)sc}$, and characteristic impedance $Z_0 = \sqrt{\frac{R+sL}{sC}}$; $r = \frac{R}{h}, l = \frac{L}{h}, c = \frac{C}{h}$ are resistance, inductance, and capacitance per unit length and h is the length of the line. To compute the RLC line response from the transfer function, the method of Padé approximation has been used by, e.g., [PR90, MA90]. The output transfer function is expanded into a Maclaurin series of s around $s = 0$, and the series is truncated to necessary order. The work of [LK92] used a recursive convolution based approach and expanded the admittance and the propagation coefficient term around $s = \infty$. In general, analytical computation of the exact voltage response is very tedious and is usually in the form of an infinite series. However, the delay estimates for RLC lines can be computed using approximate analytical formulas. Such formulas are derived by first considering a single interconnect line with source and load impedances; the delay formula for an interconnect tree can be derived by recursively using the formula for a single line. Simple analytical approaches such as Elmore delay [Elm48] and single pole delay estimates of [Sak83, Hor84, Sak93] have been widely used (these previous formulas were derived assuming resistive source impedance and capacitive load impedance).

Elmore delay is defined to be the first moment of the system impulse response, i.e., the coefficient of s in the system transfer function $H(s)$. Applying this definition to $H(s)$ in Equation (1), the Elmore delay for a distributed RLC line is

$$T_{ED} = \frac{RC}{2} + R_S C_T + R_S C + R C_T \tag{2}$$

i.e., the same as for the RC line. By considering only one pole in the transfer function, i.e, approximating the denominator polynomial to only first moment, the single pole response can be obtained [Hor84]. The single pole of the transfer function is equal to the inverse of the Elmore delay T_{ED}. Hence, the delay at arbitrary thresholds of the single pole response can be directly

related to Elmore delay (Elmore delay actually corresponds to the 63.2% threshold voltage of the single pole response). For example, delay at 90% threshold voltage is $T_{0.9} = 2.3T_{ED}$, i.e.,

$$T_{0.9} = 1.15RC + 2.3\left(R_S C_T + RC(\frac{R_S}{R} + \frac{C_T}{C})\right) \quad (3)$$

Sakurai [Sak83] also gave the response and delay calculations for the distributed RC line. He calculates the time-domain response from the transfer function using the Heaviside expansion over poles of the transfer function. Then, he approximates the response using a single pole and observes the variation of delay with respect to source and load parameters; the 90% threshold delay is *heuristically* obtained as

$$T_{0.9}(h) = 1.02RC + 2.3\left(R_S C_T + RC(\frac{R_S}{R} + \frac{C_T}{C})\right)$$

Again, these single pole delay estimates cannot accurately estimate the delay for RLC interconnect trees. Recently, Zhou et al. [ZSTGC94] proposed a two-pole approximation for the transfer function to compute the response at the load for RLC interconnection trees. However, this technique is based on response computation and does not provide any analytical expression for delay; it cannot be directly used in iterative optimization of layout. We now develop an accurate analytical model which is based on higher moments and which can capture the effects of inductance for RLC lines.

3 The New Delay Model

The previous section discussed the Elmore delay model and single- and two-pole approximations of signal delay at arbitrary threshold and at an arbitrary location x on the line. Both the Elmore model, and the models obtained from single-pole analyses, are functions of only the coefficients a_1 and b_1, i.e., they reflect only RC terms and do not capture variations in delay due to inductance of the line. This section presents a "New Delay" model which gives a closed-form delay estimate that considers the effect of inductance. To the best of our knowledge, this is the first analytical delay model for arbitrary threshold voltages which incorporates the effects of inductance of a distributed line; two example practical applications are noted in Section 4 below. We give experimental confirmations in the form of 90% threshold delay estimates which are compared against SPICE output;[1] of course, the method can be extended to any other

[1] SPICE simulation results are obtained using SPICE3 and the built-in LTRA (lossy transmission line) model.

threshold delays. For clarity of development, and to allow easier comparison with previous works, we consider capacitive loads only. However, the New Delay model can be applied to arbitrary interconnection networks by extending the analysis to the distributed lines with general load [KM94].

3.1 The Main Analysis

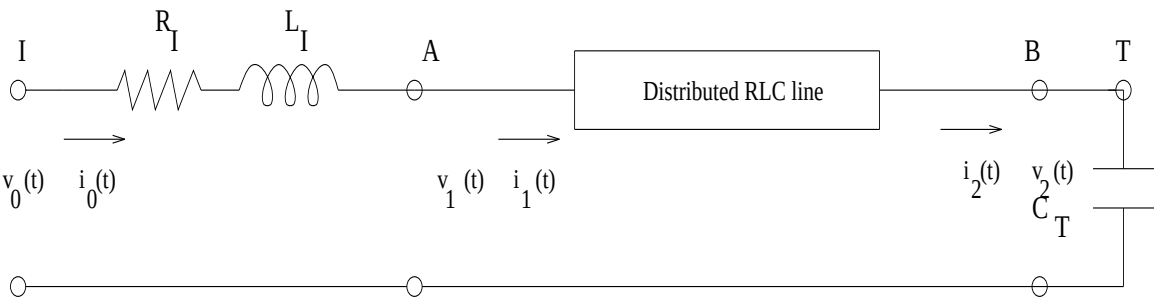

Figure 3: 2-port model of a distributed RLC line with source impedance Z_I.

Our main analysis is based on a two-pole approximation. We may model an interconnect line in a routing tree as follows. First, the interconnect line generally has source resistance and inductance equal to the resistance and inductance of the main path from source to the interconnect line. Second, the load at the end of the interconnect line can generally be approximated by the lumped capacitance of the subtree. The transfer function for the interconnect model shown in Figure 3 is

$$H(s) = \frac{1}{\cosh(\theta h)\left(1 + \frac{Z_I}{Z_T}\right) + \sinh(\theta h)\left(\frac{Z_I}{Z_0} + \frac{Z_0}{Z_T}\right)}$$

where $Z_T = \frac{1}{sC_T}$, $Z_I = R_I + sL_I$, $Z_0 = \sqrt{\frac{R+sL}{sC}}$ and $\theta h = \sqrt{(R+sL)sC}$. Expanding $cosh$ and $sinh$ as infinite series and collecting terms up to the coefficient of s^2 in the denominator, we obtain

$$\begin{aligned} H(s) &= \frac{1}{(1 + sC_TR_I + s^2L_IC_T)\cdot\left(1 + s\frac{RC}{2} + s^2(\frac{LC}{2} + \frac{(RC)^2}{24}) + \ldots\right)} \\ &\quad \overline{+\left((R_I + sL_I)\sqrt{\frac{sC}{R+sL}} + sC_T\sqrt{\frac{R+sL}{sC}}\right)\cdot\left(\sqrt{(R+sL)sC} + \frac{((R+sL)sC)^{3/2}}{6} + \ldots\right)} \\ &= \frac{1}{1 + s\left(R_IC + R_IC_T + \frac{RC}{2} + RC_T\right)} \\ &\quad \overline{+s^2\left(\frac{R_IRC^2}{6} + \frac{R_IRCC_T}{2} + \frac{(RC)^2}{24} + \frac{R^2CC_T}{6} + L_IC + L_IC_T + \frac{LC}{2} + LC_T\right) + \ldots} \end{aligned}$$

Therefore,

$$\begin{aligned} b_1 &= R_I C + R_I C_T + \frac{RC}{2} + RC_T \\ b_2 &= \frac{R_I RC^2}{6} + \frac{R_I RCC_T}{2} + \frac{(RC)^2}{24} + \frac{R^2 CC_T}{6} + L_I C + L_I C_T + \frac{LC}{2} + LC_T \end{aligned} \quad (4)$$

Recall that the transfer function for a distributed RLC line with capacitive load and ideal source is[2]

$$\begin{aligned} H(s) &= \frac{1}{cosh(\theta h) + \frac{Z_0}{Z_T} \cdot \sinh(\theta h)} \\ &= \frac{1}{1 + s(\frac{RC}{2} + RC_T) + s^2(\frac{(RC)^2}{24} + \frac{R^2 CC_T}{6} + \frac{LC}{2} + LC_T) + \ldots} \end{aligned}$$

and the coefficients are

$$b_1 = R(\frac{C}{2} + C_T) \; ; \quad b_2 = \frac{R^2 C}{6}(\frac{C}{4} + C_T) + L(\frac{C}{2} + C_T)$$

From the coefficients b_1 and b_2, the first and second moment of the transfer function can be obtained as $M_1 = b_1$ and $M_2 = b_1^2 - b_2$. Depending on the sign of $4M_2 - 3M_1^2$, the poles of the transfer function can be either real or complex. We will now separately derive the delay model from the two-pole response for each of these two cases.

Real Poles:

The two-pole methodology yields the following response for the case of real poles:

$$v(t) = V_0(1 - \frac{s_2}{s_2 - s_1} e^{s_1 t} + \frac{s_1}{s_2 - s_1} e^{s_2 t})$$

where

$$s_{1,2} = \frac{2}{-M_1 \pm \sqrt{4M_2 - 3M_1^2}} = \frac{-b_1 \pm \sqrt{b_1^2 - 4b_2}}{2b_2}$$

The condition for the poles to be real is $\sqrt{4M_2 - 3M_1^2} = \sqrt{b_1^2 - 4b_2} \geq 0$. Since $s_2 - s_1 = -\frac{\sqrt{b_1^2 - 4b_2}}{b_2}$ is negative, the coefficients $\frac{s_2}{s_2 - s_1}$ and $\frac{s_1}{s_2 - s_1}$ are positive. Also, since the magnitude $|s_2|$ is greater than $|s_1|$, the second term in the time-domain response decreases rapidly compared to the first term. Hence, the two-pole response can be approximated (lower-bounded) as

$$v(t) \approx V_0(1 - \frac{s_2}{s_2 - s_1} e^{s_1 t})$$

[2]For an open-ended line, substitute $C_T = 0$ in the coefficient equations.

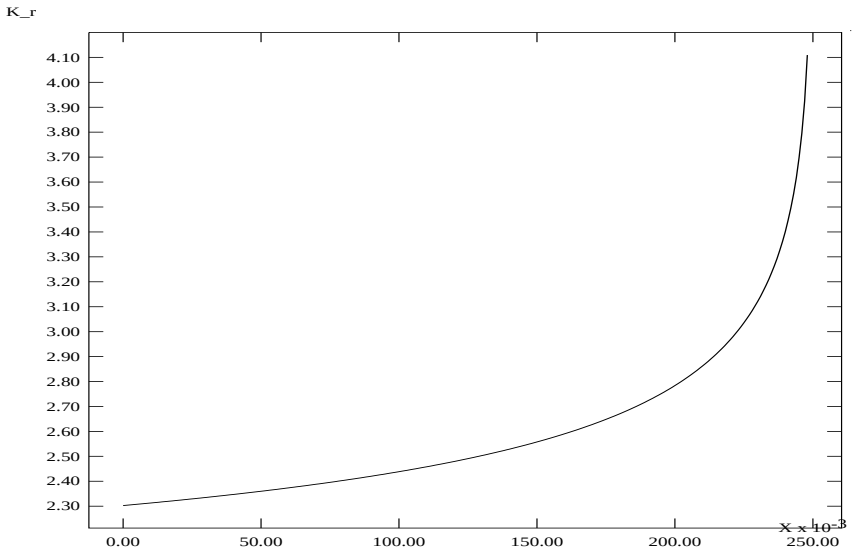

Figure 4: The variation of K_r with respect to the ratio $X = \frac{b_2}{b_1^2}$.

Since the voltage is lower-bounded, the delay obtained is an upper bound on the actual delay. The delay at v_{th} threshold voltage can be obtained as

$$s_1\tau_r = \ln\left(\frac{(s_2 - s_1)(1 - v_{th})}{s_2}\right) = -\ln\left[\frac{1}{2(1 - v_{th})}\left(1 + \frac{b_1}{\sqrt{b_1^2 - 4b_2}}\right)\right]$$

Letting

$$K_r = \ln\left[\frac{1}{2(1 - v_{th})}\left(1 + \frac{b_1}{\sqrt{b_1^2 - 4b_2}}\right)\right]$$

we have

$$\tau_r \quad = \quad \frac{K_r}{|s_1|} = K_r\frac{-M_1 \pm \sqrt{4M_2 - 3M_1^2}}{2} = K_r\frac{2b_2}{b_1 - \sqrt{b_1^2 - 4b_2}}$$

i.e., the constant K_r is a function of the coefficients b_1 and b_2. For example, at $0.9V_0$ threshold voltage the constant reduces to

$$K_r = \ln\left(5[1 + \frac{b_1}{\sqrt{b_1^2 - 4b_2}}]\right)$$

Figure 4 shows the possible variation of K_r with the quantity $X = \frac{b_2}{b_1^2}$. For the (wide) range of source, load and interconnect parameter values considered in our simulations (see Table 1), we find that K_r is actually almost a constant: Figure 5 shows the linear regression used to find

Source		Load	Delay from Response		Analytical Delay Models		
R_S	L_S	C_T	**SPICE**	**Two-pole**	**Elmore**	**New Delay (s $\times 10^{-12}$)**	
ohms	**H** $\times 10^{-12}$	**F** $\times 10^{-12}$	**s** $\times 10^{-12}$	**s** $\times 10^{-12}$	**s** $\times 10^{-12}$	**Model 1**	**Model 2**
50	2.46	0.176	22.33	22.75	22.93	22.21	21.71
100	2.46	0.176	45.30	46.26	45.20	45.70	44.60
500	2.46	0.176	224.50	227.6	223.50	228.95	223.38
1000	2.46	0.176	446.20	455.0	446.4	457.46	446.33
50	24.6	0.176	21.90	22.50	22.93	21.00	20.63
100	24.6	0.176	44.80	45.50	45.20	45.17	44.08
500	24.6	0.176	223.90	225.50	223.50	228.84	223.28
1000	24.6	0.176	446.70	452.50	446.40	457.41	446.28
25	2.46	1.76	107.10	106.90	108.40	108.65	106.04
50	2.46	1.76	210.10	212.50	210.80	214.74	209.53
100	2.46	1.76	415.20	422.50	415.40	425.10	414.76
500	2.46	1.76	2052.60	2103.0	2053.0	2103.68	2052.49
1000	2.46	1.76	4099.50	4195.5	4099.0	4201.30	4099.18

Table 1: Real Poles. The interconnect line parameters are: $R = 1.5$ ohms, $L = 2.46 \times 10^{-11}$ henry and $C = 17.6 \times 10^{-15}$ farads. Here we present only combinations of source and load parameters for which the poles of the response are real (e.g., using the lower value $R_S = 25$ ohms in lines 1 and 5 of the table would yield complex poles). The constant factor used in the **New Delay** model from two-poles is $K_r = 2.36$. The delay estimates refer to 90% threshold voltage.

the value $K_r = 2.36$ which gives the best fit between SPICE delay values and $\frac{1}{|s_1|}$. Thus, we use

$$\tau_r = 2.36 \frac{2b_2}{b_1 - \sqrt{b_1^2 - 4b_2}} \tag{5}$$

and the resultant delay estimates (denoted as New Delay Model 1) are compared against those of various other methods in Table 1. The Model 2 shown in the table refers to delay formula derived using single dominant pole analysis and is later in this section.

Complex Poles

The condition for complex poles is $\sqrt{4M_2 - 3M_1^2} = \sqrt{b_1^2 - 4b_2} \leq 0$. The time-domain response for complex poles is given by

$$v(t) = V_0 \left(1 - \frac{\sqrt{\alpha^2 + \beta^2}}{\beta} e^{-\alpha t} * \sin(\beta t + \rho) \right)$$

Note for review: The standard two-pole analysis is given for reference in Addendum 2 (not part of the submission).

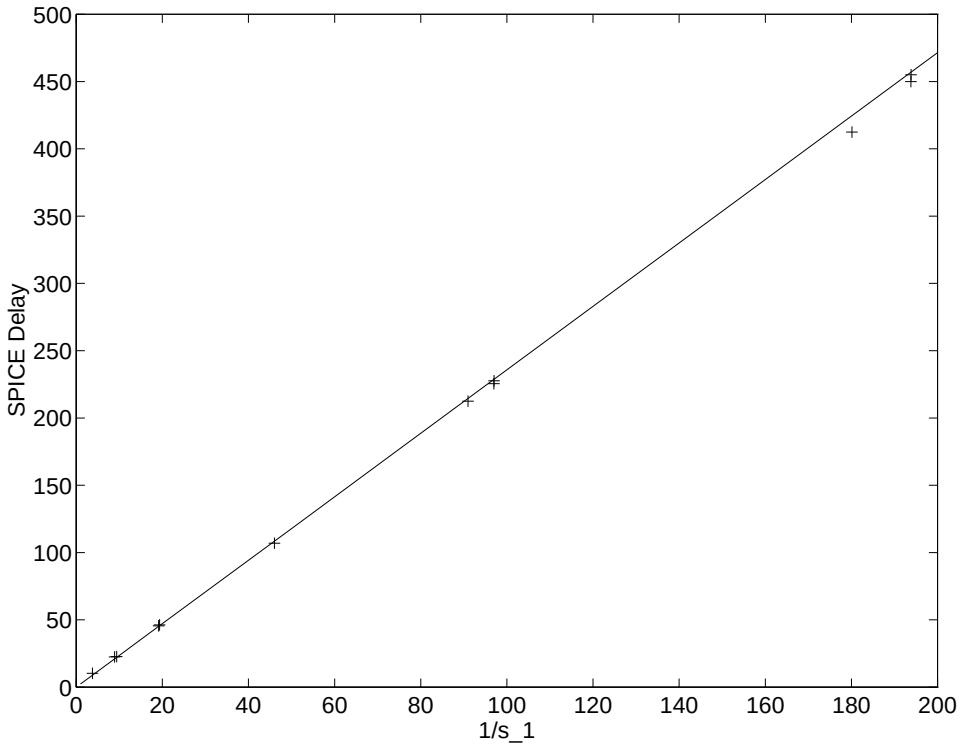

Figure 5: Linear fit between SPICE delay and $\frac{1}{|s_1|}$. The constant $K_r = 2.36$.

where $\rho = \tan^{-1}(\frac{\beta}{\alpha})$ and

$$\alpha = \frac{M_1}{2(M_1^2 - M_2)}; \quad \beta = \frac{\sqrt{3M_1^2 - 4M_2}}{2(M_1^2 - M_2)}.$$

Evaluating the above equation using the threshold voltage v_{th}, we get

$$e^{-\alpha t} * \sin(\beta * t + \rho) = \frac{1 - v_{th}}{\sqrt{1 + (\frac{\alpha}{\beta})^2}} \tag{6}$$

The delay at a given threshold voltage can be computed by solving for time in Equation (6) recursively. One way to solve the recursive Equation (6) is to approximate the time variable in the exponential term by Elmore delay, i.e., substitute T_{ED} for time t. Expanding *sine* as a Taylor series and considering only the first term yields

$$e^{-\alpha * T_{ED}} * \sin(\beta * \tau_c + \rho) \approx \frac{1 - v_{th}}{\sqrt{1 + (\frac{\alpha}{\beta})^2}}$$

$$e^{-\alpha * T_{ED}} * (\beta * \tau_c + \rho) \approx \frac{1 - v_{th}}{\sqrt{1 + (\frac{\alpha}{\beta})^2}}$$

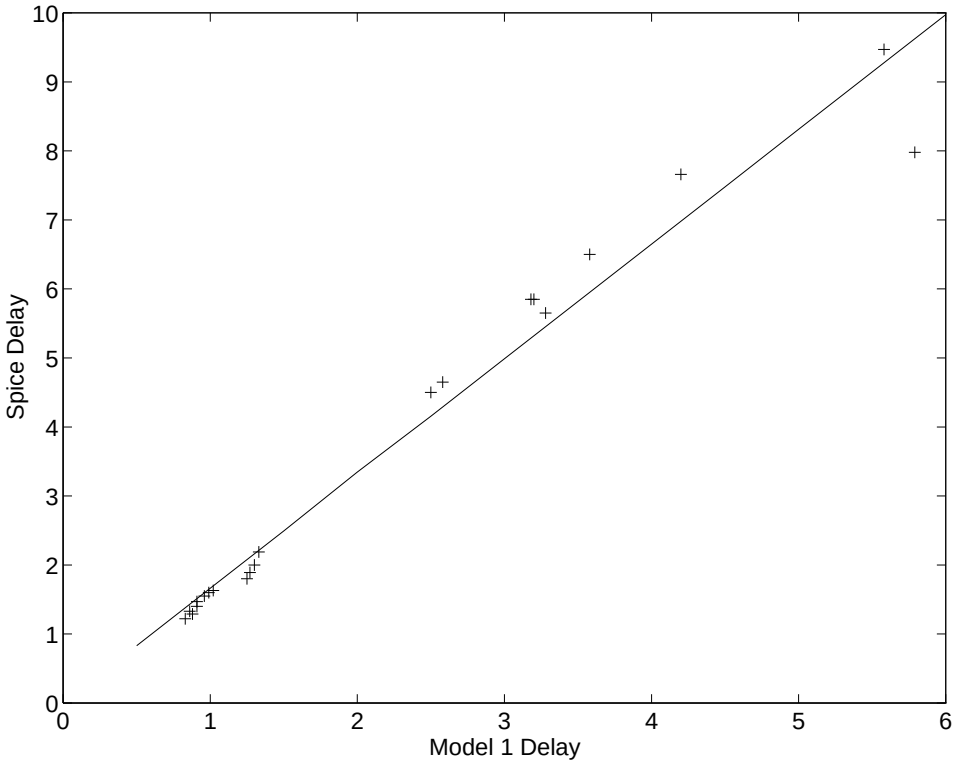

Figure 6: Linear fit between SPICE delay and $\frac{1}{\beta}$. The constant $K_{c1} = 1.66$.

Therefore,

$$\tau_c = \frac{K_{c1}}{\beta}$$

where $K_{c1} = \left(\frac{(1-v_{th})e^{\alpha * T_{ED}}}{\sqrt{1+(\frac{\alpha}{\beta})^2}} - \rho \right)$. Substituting for β and using $M_1 = b_1$ and $M_2 = b_1^2 - b_2$, we obtain

$$\beta = \frac{\sqrt{3M_1^2 - 4M_2}}{2(M_1^2 - M_2)} = \frac{\sqrt{4b_2 - b_1^2}}{2b_2}$$

Hence, our delay estimate is given by

$$\tau_c = \frac{K_{c1}}{\beta} = K_{c1} * \frac{2b_2}{\sqrt{4b_2 - b_1^2}}$$

Even though K_c is function of b_1 and b_2 for wide range of interconnect, source, and load parameters it is almost a constant. The constant value $K_{c1} = 1.66$ is again determined by finding a good fit between SPICE delay values and $\frac{1}{\beta}$, as shown in Figure 6. We thus use

$$\tau_c = 1.66 * \frac{2b_2}{\sqrt{4b_2 - b_1^2}} \tag{7}$$

Source		Load	Delay from Response		Analytical Delay Models			
R_S	L_S	C_T	**SPICE**	**Two-pole**	**Elmore**	**New Delay (s $\times 10^{-12}$)**		
ohms	**H** $\times 10^{-12}$	**F** $\times 10^{-12}$	**s** $\times 10^{-12}$	**s** $\times 10^{-12}$	**s** $\times 10^{-12}$	**Model 1**	**Model 2**	**Model 3**
10	0.0246	0.0176	1.22	1.39	0.90	1.38	2.47	1.2
15	0.0246	0.0176	1.33	1.51	1.31	1.43	2.28	1.38
20	0.0246	0.0176	1.47	1.66	1.71	1.51	2.01	1.55
25	0.0246	0.0176	1.60	1.84	2.12	1.64	1.58	1.73
10	0.0246	0.176	4.50	4.63	5.10	4.15	4.75	4.35
15	0.0246	0.176	5.85	5.94	7.32	5.31	2.24	5.32
20*	0.0246	0.176	7.90	8.00	9.55	8.64	6.52	6.29
10	2.46	0.0176	1.29	1.47	0.90	1.47	2.65	1.25
15	2.46	0.0176	1.40	1.58	1.31	1.51	2.48	1.43
20	2.46	0.0176	1.55	1.72	1.71	1.59	2.22	1.61
25	2.46	0.0176	1.63	1.90	2.11	1.69	1.85	1.78
10	2.46	0.176	4.65	4.75	5.10	4.28	5.25	4.46
15	2.46	0.176	5.85	5.98	7.33	5.28	7.14	5.43
20	2.46	0.176	7.98	7.90	9.55	9.61	6.12	6.40
10	24.6	0.0176	1.80	2.00	0.90	2.08	3.90	1.62
15	24.6	0.0176	1.89	2.10	1.31	2.10	3.79	1.80
20	24.6	0.0176	2.00	2.22	1.71	2.15	3.63	1.98
25	24.6	0.0176	2.19	2.34	2.11	2.21	3.42	2.15
10	24.6	0.176	5.65	5.75	5.10	5.44	8.54	5.27
15	24.6	0.176	6.50	6.63	7.33	5.95	6.74	6.24
20	24.6	0.176	7.66	7.85	9.55	6.97	2.82	7.21
25	24.6	0.176	9.47	9.60	11.78	9.26	6.28	8.18

Table 2: Complex Poles. The interconnect line parameters are: $R = 1.5$ ohms, $L = 2.46 \times 10^{-11}$ henry and $C = 17.6 \times 10^{-15}$ farads. Here we present only combinations of source and load parameters for which the poles of the response are complex (e.g., using the higher value $R_S = 25$ ohms in Lines 7 and 14 of the table would yield real poles). The constant factor used in the **New Delay Model 1** is $K_{c1} = 1.66$. The delay estimates refer to 90% threshold voltage.
(* Note that the estimate in Line 7 is obtained using the double pole delay expression, and is very close to the domain of real poles, which occur at $R_S \approx 20.5$ ohms.)

Table 2 shows delay values for various combinations of source, load and interconnect parameters assuming this value of K_{c1} obtained by this regression analysis (denoted as New Delay Model 1). The results show a quite close fit to SPICE delay computations.

Double Poles

The condition for a double pole is $b_1^2 = 4b_2$, i.e., $L = \frac{R^2C}{24}$. The double-pole response is

$$V(s) = \frac{V_0}{s}\frac{1}{1+b_1 s+b_2 s^2} = \frac{V_0}{s}\frac{1}{b_2(s-s_1)^2} = V_0\left(\frac{1}{s} - \frac{1}{s-s_1} - \frac{2}{b_1}\frac{1}{(s-s_1)^2}\right)$$

where $s_1 = -\frac{b_1}{2b_2}$, and the time-domain response is given by $v(t) = V_0\left(1 - e^{ts_1} - \frac{2t}{b_1}e^{ts_1}\right)$. The delay at 90% threshold is obtained as

$$\tau_{0.9} = \frac{2b_2}{b_1}\ln\left(10(1+\frac{2T_{0.9}}{b_1})\right) = K_d\frac{2b_2}{b_1} = K_d\frac{b_1}{2}$$

which gives a recursive equation for K_d, i.e.,

$$K_d = \ln\left(10(1+\frac{2T_{0.9}}{b_1}\right) = \ln\left(10(1+K_d)\right)$$

from which $K_d \approx 3.9$. Thus, in the case of a double pole the 90% threshold delay is estimated as

$$\tau_{0.9} = 3.9\frac{2b_2}{b_1} = 1.95b_1 \tag{8}$$

which is independent of the inductance value.

3.2 Single Dominant Pole Analysis

For completeness, we close this section by proposing a method to approximate the two-pole transfer function by using *single dominant pole*, as derived in the Appendix. The two poles in terms of the coefficients b_1, b_2 is

$$s_{1,2} = \frac{2}{-M_1 \pm \sqrt{4M_2 - 3M_1^2}} = \frac{-b_1 \pm \sqrt{b_1^2 - 4b_2}}{2b_2}$$

Substituting for s_1 and s_2 in terms of the coefficients b_1, b_2 in the Equation (12) we get

$$\frac{1}{p^2} = \frac{1}{s_1^2} + \frac{1}{s_1^2} = \frac{4b_2^2}{(-b_1+\sqrt{b_1^2-4b_2})^2} + \frac{4b_2^2}{(-b_1-\sqrt{b_1^2-4b_2})^2} = (b_1^2 - 2b_2)$$

Therefore, the single dominant pole is

$$p = \frac{1}{\sqrt{(b_1^2-2b_2)}}$$

and the delay at $0.9V_0$ threshold can be estimated using Equation (13) as

$$\tau_p = 2.3\sqrt{(b_1^2-2b_2)} \tag{9}$$

Even though this delay model is derived assuming real poles, we use the same model even for complex poles to calculate the delay by considering the absolute value of $(b_1^2 - 2b_2)$, i.e.,

$$\tau_p = 2.3\sqrt{|(b_1^2 - 2b_2)|}$$

We refer to this delay expression as **New Delay Model 2**. The delay estimates for various configurations of source, load and interconnect line parameters are given in Table 1 (real poles) and Table 2 (complex poles). It is clear that for real poles, both Elmore delay and the two-pole / single dominant-pole **New Delay** estimates (all of which are analytical models) are very close to SPICE-computed delay (which is derived from a computed response). For higher source impedances, the single dominant-pole delay estimate is almost identical to Elmore delay, since the effect of coefficient b_2 on the delay is much smaller than that of coefficient b_1. The advantage of the two-pole and the single dominant-pole **New Delay** models is that they incorporate inductance parameters of both the source and the interconnect line. This is useful in such layout optimization problems as gate/wire sizing, which has traditionally been based only on RC delay models.

For complex poles (Table 2), in the worst case the Elmore delay model estimates can be off by up to 50% over the range of parameter values studied. However, the **New Delay** model estimates are again very close to SPICE-computed delays. We believe that these experimental results indicate that the New Delay model can accurately predict interconnect delays based on resistance, capacitance and inductance effects.

3.3 Intutive Delay Model

A simple way to obtain a delay model to incorporate the inductive and higher order effects is by using the first moment and the standard deviation of the response. To obtain an expression for delay using both coefficients b_1 and b_2 is by approximating the delay as the sum of first moment (M_1, which is Elmore delay) and the standard deviation (σ) from the first moment, i.e.,

$$\tau_{approx} = K(M_1 + \sigma) = K(M_1 + \sqrt{M_1^2 - M_2}) = K(b_1 + \sqrt{b_2})$$

From the above discussion we find that the constant K depends on whether the poles are real or complex. When the poles are real, the contribution of coefficient b_2 is much smaller than that

of b_1, and the model is similar to Elmore delay; thus, we may use $K = 2.3$. If the contribution of coefficient b_2 is comparable to that of b_1, it turns out that the constant K is close to one ($K = 1.0$). We thus have:

$$\begin{aligned} \tau_{approx}(i) &= 2.3(b_1 + \sqrt{b_2}) \quad \text{for Real poles} \\ &= 1.0(b_1 + \sqrt{b_2}) \quad \text{for Complex poles} \end{aligned}$$

This model is referred as **Model 3** in the comparison of various delay models. Experimental results for the same range of parameter values as in the Tables indicate that even this intuitive model is quite good for complex poles, and for real poles it has a maximum error of 30%. The results for the complex pole configurations are shown in Table 2. From these comparison of various delay models we conclude that **New Delay Model 1** can accurately predict the delays for various interconnect parameters.

4 Two Example Applications

In this section, we present two applications of the New Delay model developed in the previous section. The first application extends the New Delay model to arbitrary interconnection trees; the second application is to the reduction of threshold delay by introducing ringing (without false switching) in the output response. While this is not central to our contribution, we include this discussion to give an indication of the range of applications for the preceding analyses.

4.1 Interconnect Trees

An RLC network is called an RLC tree if it does not contain a closed path of resistors and inductors, i.e., all resistors and inductors are floating with respect to ground and all capacitors are connected to ground [Wya87]. We now consider RLC trees where each edge is modeled using distributed RLC 2-port parameters. Consider the voltage response and delay at an arbitrary output node k. The path from source S (root of the tree) to node k is denoted by $p(k)$ and is referred as the *main path*. The edges/nodes not on the main path are the *off-path* edges/nodes. Elmore delay at node k for RC interconnect trees [RPH83, BKR93] is given by

$$T_{ED}(k) = R_S C_{T(S)} + \sum_{\forall i \in p(k)} R_i (\frac{C_i}{2} + C_{T(i)})$$

where $T(S)$ is the tree rooted at source S, $T(i)$ is the subtree rooted at node i, R_S is the source resistance, and $C_{T(i)}$ is the total capacitance of the subtree rooted at node i. This model is widely used for interconnect tree analysis and synthesis, but since it cannot take into account the inductance of the interconnect line, the delay estimation may not be accurate and the trees synthesized could be sub-optimal. Using the New Delay model, we can obtain a new delay estimate for RLC interconnect trees, namely,

$$T_{0.9}(k) = \sum_{\forall i \in p(k)} \tau_{rc}(i)$$

where $\tau_{rc}(i)$ indicates the 90% threshold delay for distributed RLC line with capacitive load for the two cases depending on the whether the poles are real or complex for the tree edge i.

$$\begin{aligned} \tau_{rcd}(i) &= 2.36 \cdot \frac{2b_2}{b_1 - \sqrt{b_1^2 - 4b_2}} \quad \text{for Real poles} \\ &= 1.66 \cdot \frac{2b_2}{\sqrt{4b_2 - b_1^2}} \quad \text{for Complex poles} \\ &= 1.95 \cdot b_1 \qquad\qquad \text{for Double poles} \end{aligned}$$

where b_1 and b_2 are given by Equation (4).

4.2 Constraint on First and Second Moment for Minimum Delay

For interconnect synthesis, finding parameters of interconnect and driver sizing for optimum delay can be achieved via a simple analytic constraint. Consider a simple RLC line driven by a gate, with Z_S being the driver impedance and C_L being the load capacitance at the end of the line as shown in Figure 2. The characteristic impedance of the line is given by, $Z_0 = \sqrt{\frac{R+sL}{sC}}$. Ideally, the driver and line parameters are adjusted such that Z_S matches Z_0 and the voltage response at the end of the line is critically damped.[3] However, if the driver impedance Z_S is just smaller than the characteristic impedance of the line, the voltage response will have a small amount of ringing – which can be advantageous in that the delay time to reach the threshold voltage will decrease [YB94]. Of course, the problem with ringing is that it can cause false switching if the voltage response drops back below the threshold. However, if the maximum oscillation peak (overshoot or undershoot) is constrained such that false switching does not occur, then the advantages of ringing can be exploited. We now show an analytical equation,

[3] At least, the magnitudes of both should be made equal.

in terms of moments or coefficients of the transfer function, for maximum undershoot with no false switching. The voltage response for ringing is given by

$$v_{out}(t) = V_0 \left[1 - \frac{\sqrt{\alpha^2 + \beta^2}}{\beta} e^{-\alpha t} sin(\beta t + \rho) \right]$$

where $\rho = tan^{-1}(\frac{\beta}{\alpha})$. To find the location of overshoot and undershoot in the response make $\frac{\partial v(t)}{\partial t} = 0$, which yields $\beta t = n\pi$, with $n = 1, 3, 5, \ldots$ for overshoot locations and $n = 2, 4, 6, \ldots$ for undershoot locations. Therefore, the first undershoot occurs at time $T_1 = \frac{2\pi}{\beta}$, and the value of the undershoot is given by

$$\Delta v = V_0 e^{-\alpha T_1} \sqrt{1 + (\frac{\alpha}{\beta})^2} sin(\beta T_1 + \rho) = V_0 e^{-\alpha T_1}.$$

The constraint for a given percentage undershoot, v_{us}, can be obtained as

$$\frac{\alpha}{\beta} = \frac{1}{2\pi} \cdot |\ln(v_{us})|$$

For example, with 5% undershoot we have $v_{us} = 0.05 V_0$ and $\frac{\alpha}{\beta} = 0.48$. We can express α and β in terms of moments and coefficients of the transfer function, i.e.,

$$\frac{\alpha}{\beta} = \frac{M_1}{\sqrt{3M_1^2 - 4M_2}} = \frac{b_1}{\sqrt{4b_2 - b_1^2}}$$

Therefore,

$$M_1^2 = \left[\frac{4(\frac{\alpha}{\beta})^2}{3(\frac{\alpha}{\beta})^2 - 1} \right] M_2 \tag{10}$$

and

$$b_1^2 = \left[\frac{4(\frac{\alpha}{\beta})^2}{(\frac{\alpha}{\beta})^2 + 1} \right] b_2 \tag{11}$$

With 5% undershoot Equations (10) and (11) reduce to

$$M_1^2 = -2.86 \cdot M_2 \ ; \quad b_1^2 = 0.74 \cdot b_2$$

and the 90% threshold delay for this case can be obtained as

$$T_{0.9} = 1.66 \cdot \frac{2b_2}{\sqrt{4b_2 - b_1^2}} = 2.13 b_1$$

Similarly, for 5% overshoot the relation between moments and coefficients is

$$M_1^2 = 2.11 \cdot M_2 \ ; \quad b_1^2 = 1.91 \cdot b_2$$

Therefore, the corresponding delay is

$$T_{0.9} = 1.20 b_1$$

As expected, we observe that the delay increases for a strong undershoot requirement, and in general delay will increase if ringing in the response is suppressed [YB94]. Using the constraints on b_1 and b_2, delay-driven routing tree construction can be performed.

5 Conclusions

We present a New Delay model for distributed RLC lines which is based on either a two-pole analysis or a single dominant-pole analysis, and which considers the effect of inductance (unlike previous analytical delay estimates such as Elmore delay). We give example applications of the New Delay model to the analysis of general interconnection trees and to delay minimization by controlled ringing. We are currently extending our techniques into a unified methodology for response and delay estimation in distributed $RLCG$ interconnect structures [KM94]. We are also working on extending these techniques for stable signal propagation [FC92] considering time-of-flight in the delay estimation. Finally, we are in the process of incorporating our New Delay model for delay-driven routing tree construction, zero-skew routing, and delay estimation in nets spanning multiple routing layers (via modeling).

References

[BKR93] K. D. Boese, A. B. Kahng and G. Robins, "High-Performance Routing Trees With Identified Critical Sinks", *Proc. 30th ACM/IEEE Design Automation Conf.*, June 1993, pp. 182-187.

[Dwo79] L. N. Dworsky, *Modern Transmission Line Theory and Applications*, Wiley, 1979.

[Elm48] W. C. Elmore, "The Transient Response of Damped Linear Networks with Particular Regard to Wideband Amplifiers", *Journal of Applied Physics* 19, Jan. 1948, pp. 55-63.

[FC92] R. C. Frye and H. Z. Chen, "Optimal Self-Damped Lossy Transmission Line Interconnections for Multichip Modules", *IEEE Trans. on Circuits and Systems-II*, Nov. 1992, pp. 765-771.

[Hor84] M. A. Horowitz, "Timing Models for MOS Circuits", *PhD Thesis*, Stanford University, Jan. 1984.

[KM94] A. B. Kahng and S. Muddu, "A General Methodology for Response and Delay Computations in VLSI Interconnects", *UCLA CS Dept. TR-940015*, March 1994.

[LK92] S. Lin and E. S. Kuh, "Transient Simulation of Lossy Interconnect", *Proc. 29th ACM/IEEE Design Automation Conf.*, June 1992, pp. 81-86.

[MA90] S. P. McCormick and J. Allen, " Waveform Moment Methods for Improved Interconnection Analysis", *Proc. 27th ACM/IEEE Design Automation Conf.*, June 1990, pp. 406-412.

[Mil79] J. Millman, *Microelectronics - Digital and Analog Circuits and Systems*, McGraw-Hill, 1979.

[PR90] L. T. Pillage and R. A. Rohrer, "Asymptotic Waveform Evaluation for Timing Analysis", *IEEE Trans. CAD*, Apr. 1990, pp.352-366.

[RBR92] V. Raghavan, J. E. Bracken and R. A. Rohrer, "AWESpice: A General Tool for the Accurate and Efficient Simulation of Interconnect Problems", *Proc. 29th ACM/IEEE Design Automation Conf.*, June 1992, pp. 87-92.

[RGP91] C. L. Ratzlaff, N. Gopal, and L. T. Pillage, "RICE: Rapid Interconnect Circuit Evaluator", *Proc. 28th ACM/IEEE Design Automation Conf.*, June 1991.

[RP91] J. S. Roychowdhury and D. O. Pederson, "Efficient Transient Simulation of Lossy Interconnect", *Proc. 28th ACM/IEEE Design Automation Conf.*, June 1991, pp. 740-745.

[RPH83] J. Rubinstein, P. Penfield and M. A. Horowitz, "Signal Delay in RC Tree Networks", *IEEE Trans. on CAD* 2(3), July 1983, pp. 202-211.

[Sak83] T. Sakurai, "Approximation of Wiring Delay in MOSFET LSI", *IEEE Journal of Solid-State Circuits*, Aug. 1983, Vol.18, No.4, pp. 418-426.

[Sak93] T. Sakurai, "Closed-Form Expressions for Interconnection Delay, Coupling, and Crosstalk in VLSI's", *IEEE Trans. on Electron Devices*, Jan. 1993, pp. 118-124.

[SK93] M. Sriram and S. M. Kang, "Fast Approximation of The Transient Response of Lossy Transmission Line Trees", *Proc. ACM/IEEE Design Automation Conf.*, June 1993, pp. 691-696.

[WE92] N. H. E. Weste and K. Eshraghian, *Principles of CMOS VLSI Design: A Systems Perspective*, 2nd ed., Addison-Wesley, 1992.

[Wya87] J. L. Wyatt, Jr, " Signal Propagation Delay in RC models for Interconnect", *Circuit Analysis, Simulation and Design*, Elsevier Science Publishers, 1987.

[YB94] Y. Yang and R. Brews, "Overshoot Control for Two Coupled RLC Interconnections", *IEEE Trans. Components, Packaging and Manufacturing Tech*, Aug. 1994.

[ZSTGC94] D. Zhou, S. Su, F. Tsui, D. S. Gao and J. S. Cong, "A Simplified Synthesis of Transmission Lines with A Tree Structure", *Intl. Journal of Analog Integrated Circuits and Signal Processing*, Jan. 1994, pp. 19-30.

Appendix: Calculation of Single Dominant Pole from Two-pole Transfer function

The transfer function of the system with two dominant poles is

$$H(s) = \frac{k_1}{s - s_1} + \frac{k_2}{s - s_2} = \frac{k_1 s_1 s_2}{(s - s_1)(s - s_2)} = \frac{k_1}{(1 - \frac{s}{s_1})(1 - \frac{s}{s_2})}$$

where s_1 and s_2 are the two poles of the transfer function. In trying to approximate the second order (two-pole) function with a single pole function, the main criterion used is that both transfer functions should match up to 3 dB frequency [Mil79]. The concept of 3 dB is widely used in low-pass transfer functions and refers to the fact that the magnitude at 3 dB frequency should be $\frac{1}{\sqrt{2}}$ of the magnitude at zero frequency (DC), i.e.,

$$|H_{3dB}| = \frac{k_1}{\sqrt{2}}$$

The overall transfer function magnitude (or gain) of the two-pole transfer function can be obtained by multiplying the magnitudes of individual poles. For the case of real poles, calculating the magnitude of the two-pole transfer function at $s = j\omega$ and equating to the value at 3 dB yields

$$|H(\omega)| = k_1 \cdot \frac{1}{\sqrt{1 + (\omega/s_1)^2}} \cdot \frac{1}{\sqrt{1 + (\omega/s_2)^2}} = \frac{k_1}{\sqrt{2}}$$

$$\frac{1}{\omega} = \sqrt{\frac{1}{s_1^2} + \frac{1}{s_1^2}}$$

Let the transfer function with a single dominant pole be

$$H(s) = \frac{k_3}{1 - \frac{s}{p}}.$$

Again calculating the magnitude and equating to the value at 3 dB frequency, we get

$$\frac{k_3}{\sqrt{1 + (\omega/p)^2}} = \frac{k_3}{\sqrt{2}}$$

which implies

$$p = \omega$$

and

$$\frac{1}{p} = \sqrt{\frac{1}{s_1^2} + \frac{1}{s_1^2}} \tag{12}$$

Thus, the response for a single dominant pole is given by

$$V_{out}(s) = V_0 \frac{k_3}{s(1 - \frac{s}{p})}$$

and using the boundary conditions similar to the ones described in the two-pole methodology, the time-domain response is

$$v_{out}(t) = V_0 \left[1 - e^{pt}\right]$$

Therefore, the delay at a threshold voltage v_{th} is

$$\tau_{th} = \frac{1}{|p|} \ln \left(\frac{1}{1 - v_{th}} \right) \tag{13}$$